Endohedral formation, energy transfer, and dissociation in collisions between Li + and C 60

V. Bernshtein and I. Oref

Citation: The Journal of Chemical Physics **109**, 9811 (1998); doi: 10.1063/1.477650
View online: http://dx.doi.org/10.1063/1.477650
View Table of Contents: http://scitation.aip.org/content/aip/journal/jcp/109/22?ver=pdfcov
Published by the AIP Publishing

Endohedral formation, energy transfer, and dissociation in collisions between Li^+ and C_{60}

V. Bernshtein and I. Oref[a)]
Department of Chemistry, Technion-Israel Institute of Technology, Haifa 32000, Israel

(Received 11 August 1998; accepted 2 September 1998)

Quasiclassical trajectory calculations were performed on Li^+ ion collisions with a C_{60} molecule. The probabilities of endohedral formation and escape from the cage are reported. It is found that endohedral formation depends on the relative translational energy and it is independent of the internal energy. The average energy transferred per collision of a Li^+ with a fullerene molecule is reported and its dependence on the relative translational energy is given. The collisional energy transfer probability density function, $P(E',E)$, is calculated for two translational energies and the results are used to calculate the degree of dissociation of the fullerene molecule following a collision with Li^+. Details of the intramolecular vibrational energy redistribution, IVR, are reported. It is found that following an exciting collision, energy relaxes by moving from one moiety to another within the molecule. Initial partial relaxation can be as fast as ~67 fs but total redistribution of energy takes ~1.5 ps. © *1998 American Institute of Physics.* [S0021-9606(98)01346-4]

INTRODUCTION

A major activity of current interest in the field of fullerene chemistry is the insertion of atoms and ions into the internal cavity of the spherical C_{60} molecule. The endohedral complex is denoted by $M@C_{60}$ or by $Rg@C_{60}$ where M is a metal atom and Rg is a rare gas atom or ion. Endohedral complexes are formed by binary collisions between M and C_{60} in the gas phase or by gas-surface interactions where the C_{60} forms the surface layer. Insertion can take place in thermal systems at relatively high temperatures and pressures[1] or in beams.[2] For charged particle insertion, either M or Rg are ions[2] or the C_{60} molecule is charged.[3] In the latter case the high-energy C_{60}^+ ions collide with inert gas atoms and insertion occurs.

Collisions of rare gas ions with C_{60} were studied at various collision energies.[2a–c] It was found that the dominant mechanism is charge exchange and the inert gas atom penetrates the C_{60}^+ ion to form a $Rg@C_{60}^+$ endohedral complex. The insertion efficiency is translational energy dependent and can reach values of over 1%. Collisions of alkali metals ions also lead to endohedral formations. In this case there is no charge exchange between the metal ions and the C_{60} because of the low ionization potentials of the metals.[2d,e] Insertion occurs also in collisions of accelerated noble gas ions with surface layers of C_{60}.[4a] A similar procedure was used for the insertion of alkali metal ions into C_{60}.[4b]

In parallel to the intense experimental activity, numerical calculations were done in order to explain the experimental results. *Ab initio* calculations[3e,5a,b] were performed to determine the parameters of the potential energy surface and the stability of the endohedral system. Ion/C_{60} intermolecular potentials were developed[6] and used in molecular dynamics simulations of experiments. The system[3e] C_{60}^+/He was modeled by using a modified hydrocarbon potential[6a] and the trajectories were restricted to a line of approach through the 5 and 6 member rings in the C_{60}. Good agreement between experiments and simulations was reported. Another molecular dynamics study[7] on the He^+/C_{60} and Li^+/C_{60} systems did not reproduce the insertion found in experiments.

In this work we report the results of trajectory calculations of binary collisions between Li^+ and a C_{60} molecule. The purpose is to understand the mechanism of endohedral formation by insertion through the pentagonal and hexagonal rings, to calculate its probability and to find its dependence on the internal and the relative translational energies. To find the mechanism of inelastic scattering, the average energy transferred in an ion-molecule collision, the probability for an energy transfer event, and the rate of dissociation of the collisionally excited C_{60} molecule.

THEORY

Details of the trajectory calculations

The numerical methods used in the present work are reported in Refs. 8a, 8b. The equations of motion were integrated by using a modified public domain program Venus.[8c] The intermolecular potential used is a carbon/ion pairwise potential.[6b,7] It combines the repulsive part of a Lennard-Jones potential with an ion-atom attractive part whose $1/r^4$ dependence is derived by using the Hellman–Feynman theorem;[7]

$$V_{c-\mathrm{ion}} = 4\epsilon[(\sigma_{ci}/r)^{12}/z^2 - (\sigma_{ci}/r)^4], \tag{1}$$

where $\epsilon = 78.4$ meV;[6b] $\sigma_{ci} = (\sigma_c + \sigma_{\mathrm{Li}+})/2$; $\sigma_c = 0.284$ nm, and $\sigma_{\mathrm{Li}+} = 0.136$ nm.

The intramolecular harmonic potential includes all the normal modes contributions, stretching, bending, and non-

a)Electronic mail: chroref@aluf.technion.ac.il

bonded interactions between second-neighbors atoms.[6c] A reasonable approximation is using one force constant for all the short C–C distances and one for the long C–C distances. The same approximation was used for the bendings force constants. The values of the parameters of this potential were obtained from Ref. 6c. The initial translational energy was chosen to agree with experiments. The initial rotational energy was chosen from the appropriate thermal energy distributions. The initial internal energy was varied systematically. The initial impact parameter was chosen randomly between 0 and its maximum value b_m. The value of the maximum impact parameter b_m was determined separately by determining the point at which the plot of $b\langle\Delta E\rangle$ vs $b+db$ is 0 and adding to it 0.2 nm. A value of 0.7 nm was used in the present calculations. Convergence of the average energy transferred in up and down collisions, $\langle\Delta E\rangle_{\rm up}$ and $\langle\Delta E\rangle_d$, as a function of the number of trajectories was obtained at 3000 trajectories, well below the 10 000 to 50 000 trajectories used in each run in the present study. The large number of trajectories was chosen in order to provide good statistical sampling in the binning procedure which was used to evaluate the outcome of the trajectories.

Insertion and endohedral formation was detected by filtering the trajectories and marking those with center of mass distances smaller than 0.3 nm (smaller than the C_{60} radius of 0.35 nm). Trajectories that achieved a center of mass distance smaller than 0.3 nm that increased with time were those that escaped the cage.

Calculation of energy transfer probability density function $P(E',E)$

The majority of collisions between a Li^+ ion and a C_{60} molecule do not result in an endohedral formation but in inelastic trajectories which transfer energy between the colliding pair. An inelastic collisional event results in translation to vibration/rotation energy transfer which is called an up collision whose average is denoted by $\langle\Delta E\rangle_u$, or the reverse process, a down collision, whose average is denoted by $\langle\Delta E\rangle_d$. The overall average energy transferred $\langle\Delta E\rangle_{\rm all}$, is the sum of both processes appropriately weighted.[9g] The probability of transferring a given ΔE is given by the collisional energy transfer probability density function, $P(E',E)$. Evaluation of this quantity turned out to be problematic. In principle, $P(E',E)$ is defined by the expression

$$P(E',E)=N(E',E)/N/\delta E, \tag{2}$$

where $N(E',E)$ is the number of trajectories that transfer a given ΔE between an initial value E and a final value E'. δE is the energy interval within which $N(E',E)$ is evaluated. N is the total number of trajectories and it is a function of the value of the maximum impact parameter b_m. The larger the value of b_m the larger the value of N. Thus the shape of $P(E',E)$ is b_m dependent. The choice of a particular b_m has a degree of arbitrariness in it and therefore $P(E',E)$ is not well defined. One way of solving the problem was to avoid counting the elastic collisions by defining the elastic peak as $P(\Delta E=0)=1/\delta E-\Sigma P(\Delta E\neq 0)$. This normalization procedure did not prove particularly successful since it did not remedy the problem since the value of $P(\Delta E=0)$ remained a function of b_m, therefore, the whole normalized $P(E',E)$ is a function of b_m. To alleviate the problem, a new method was proposed in Ref. 8d. The total number of trajectories is divided into two groups. In the first are those trajectories that, during the collision, undergo an intermolecular interaction which couples the ion and the molecule and cause a perturbation δ in the internal energy of the molecule which may or may not result in net ΔE exchange. The second group includes all those trajectories, which represent elastic collisions, which emanate from trajectories with such a large impact parameter that no energy exchange can possibly take place. The number of trajectories that belong to the first group, i.e., those that are effective and perturb the molecule by at least δ, are denoted by $N_{\rm eff}$.

A collision sphere, with a critical radius, r_c, is defined such that within it the energies of the bath and the molecule are coupled. In a given sample of N trajectories with any arbitrary value of b_m, there is therefore an effective number of trajectories, $N_{\rm eff}$ which fall within a cross section defined by r_c. The ratio $N_{\rm eff}/N$ is given by the ratio $(r_c/b_m)^2$. $N_{\rm eff}$ is the important quantity because it, and not N, defines the value of $P(E',E)$. In Ref. 8d, the unknown value of r_c was found, for Ar/benzene collisions, from the value of the distance of closest approach, the least minimal distance, LMD, of the bath atom to the atoms in the colliding molecule. r_c is the value of LMD above which no energy exchange takes place. For spherical molecules like C_{60}, and only for such molecules, it is possible to use center of mass coordinate system, which is easy to visualize. Therefore, in the present work, we have evaluated r_c from the distance of closest approach in the center of mass coordinate system, LCM and the results that are reported here are based on it.

The energy transfer probability density function is therefore defined by the equation

$$P(E',E)=N(E',E)/N_{\rm eff}/\delta E. \tag{3}$$

Previously,[8d] it was shown that when Eq. (3) is used, $P(E',E)$ is normalized and it also obeys detailed balance.

RESULTS AND DISCUSSION

The present work addresses the following major processes: the dynamics of insertion of a Li^+ ion into a C_{60} cage, the collisional energy transfer of those trajectories that did not insert, and the dissociation of the C_{60} molecules which were excited by collisions. Each process is explored and its dependence on system parameters such as translational and internal energies is reported. The dynamic behavior of the system depends on its intermolecular potential that affects the energy transfer process and the position of the endohedral atom inside the cage. Therefore the potential is discussed first.

The intermolecular potential

The intermolecular potential used in the calculation is a pairwise potential given by Eq. (1). The potential energy in a given trajectory is a function of the orientation of the colliding pair. A line-of-center collision through the center of the six carbon ring will have a deeper well than that of any trajectory where the atom hits, for example, a single bond

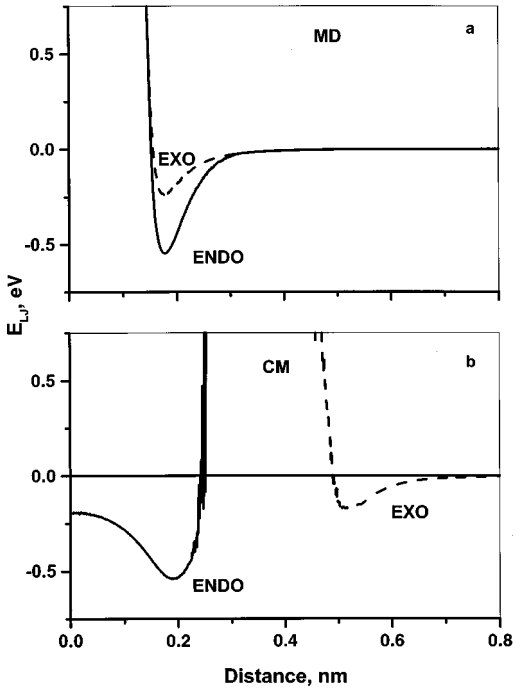

FIG. 1. The intermolecular global potential vs the distance between a Li^+ and a C_{60} molecule. Endohedral configuration (—); exohedral configuration (— — —). (a) The potential as a function of the minimal distance. (b) The potential as a function of the center of mass distance. The figures are an average of 50 000 trajectories.

between two carbon atoms, a five member ring or any other geographic location in the molecule. This is discussed and demonstrated also for collisions of Ar with a benzene molecule in Ref. 8d where it was found that the deepest potential well occurs when an Ar atom approaches the center of the benzene ring from above. It is worthwhile to define a global potential[8d] where all orientations are averaged out by averaging the potential of many trajectories, 10 000 to 50 000 in our case, with random initial conditions. Figure 1 shows the global potential inside and outside the sphere in center of mass, CM, coordinate system. The depth of the minimum outside the sphere is less than 200 meV while inside it is greater than 500 meV. The inside minimum is located 0.19 nm from the center of mass or 0.16 nm from the inside wall. The outside well is located at the same distance on the outer surface of the sphere. These values are totally different than the values of the pairwise potential used in the trajectory calculations that use a collision radius of 0.21 nm, a value much greater than reported above. The reason for the difference in values is that the location of the minimum in the global potential occurs because of simultaneous, multiple interactions with a number of carbon atoms when the ion is located symmetrically above a ring in the molecule. The differences between the pairwise potential and the global potential indicate that they are not interchangeable and caution should be used when trying to apply global potential parameters to pair-wise potentials.

Insertion of Li^+ in C_{60}

Insertion of a Li^+ ion into a C_{60} cage is affected by the relative translational energy of the colliding pair. Three energy regimes can be distinguished. The first is the very low-energy region where no insertion can possibly take place. The second is the medium energy regime where the translational energy is sufficient for insertion but it is not high enough to enable the ion to escape the cage once inside it. The third, a high-energy region, is where insertion occurs and a fraction of the ions escape the cage. Figure 2 shows the dependence of the total number of penetrations (endohedral+escape) as a function of the relative translational energy. Below 6 eV no insertion occurs. Above 6 eV insertion occurs through the hexagonal ring. This energy is not enough to penetrate a five-member ring. At the high-energy end above 20 eV, escape from the cage occurs as well. As the translational energy increases the number of atoms which escape the cage increases.

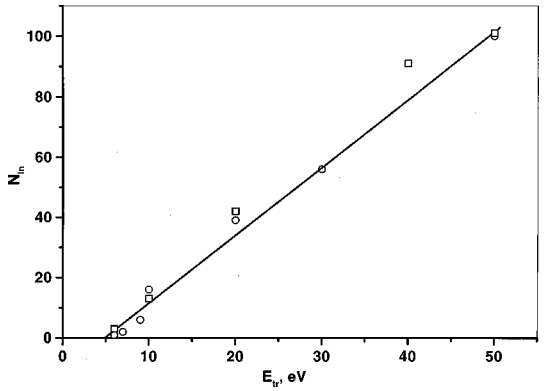

FIG. 2. The total number of $Li@C_{60}^+$ formed (including the ions that escaped the cage) as a function of the translational energy. The solid line is a best fit to the data. The total number of trajectories was 10 000 and the internal energy was 3.1 eV (□) and 26 eV (○).

The degree of insertion as a function of the translational energy is given in Table I. The 6 eV translational energy threshold for insertion agrees with the experimental findings of Wan *et al.*[2d] The penetration yield, which at 50 eV is about[2e] 1%, agrees also very well with the experimental results of Wan *et al.* The total number of penetrations with translational energy up to 50 eV can be estimated by the expression: $N=-11+2.25E_{\mathrm{tr}}$ where E_{tr} is the translational energy. This is a reliable estimate since it is based on 10 000 trajectories and calculated for all random orientations and impact parameters. Of the nonpenetrating collisions some are energy transferring collisions to which a major part of this work is devoted. The rotational temperature does not affect the number of penetrations since the rotations are much slower compared with the translations. Insertions occur on a time scale much faster than the rotation of the C_{60}. Insertion also occurs via five-member rings with threshold translational energy of 29 eV. The reason for the difference in the values of the threshold energies is that the radius of a five-member ring is too small to enable a slip-through mechanism, as is the case in a six-member ring. The harmonic potential used in the present calculations does not allow the formation of a large opening at relatively low energies. This will be remedied when an anharmonic potential will be used in future calculations.

The endohedral complex has enough energy to dissoci-

TABLE I. Degree of insertion and average energies transferred, in eV, as a function of translational energy for 10 000 trajectories for two temperatures and two values of internal energy.

E_{trans}, eV	N_{in}[a]	N_e[b]	$\langle\Delta E\rangle_{all}$	$\langle\Delta E\rangle_d$	$\langle\Delta E\rangle_{up}$
$T_{rovib}=613$ K, $E_{vib}=3.1$ eV					
6	3	-	2.24	−0.01	2.38
10	13	-	3.64	−0.01	3.88
20[c]	42	1	7.38	−0.01	7.78
40[c]	91	5	16.55	−0.01	16.74
50[d]	101	10	22.19	−0.02	22.22
$T_{rot}=1200$ K, $E_{vib}=26$ eV					
5	-	-	1.80	−0.07	2.02
6	1	-	2.16	−0.07	2.40
7	2	-	2.50	−0.06	2.79
9	6	-	3.22	−0.05	3.55
10	16	-	3.71	−0.05	4.14
20	39	1	7.38	−0.05	8.00
30	56	3	11.67	−0.06	12.31
50	100	11	22.24	−0.11	22.51

[a]Number of insertions including the number of escapes from the cage.
[b]Number of ions escaping the cage after insertion.
[c]Average of 50 000 trajectories normalized to 10 000 trajectories.
[d]Average of 20 000 trajectories normalized to 10 000 trajectories.

ate not only by the ion escaping the cage and leaving the molecule intact but also by fragmenting into a C_{58}^+ and a C_2. However, the present potential does not allow for direct calculations of the percent dissociation of the C_{60} molecule. It is possible, however, to evaluate it indirectly and this is done and discussed later on where energy transfer and dissociation will be combined to give an estimate of the degree of dissociation as a function of the internal energy. With a nonharmonic potential the dissociation channel can be evaluated directly.[2e] This work is now in progress.

Unlike translational energy, the internal energy does not contribute to penetration. Table II shows that the number of penetrations is constant regardless of the internal energy of the molecule. Since the Li^+ ion is small enough it can slip easily through the hexagonal hole. Extension of the size of the hole due to internal excitations therefore, does not affect the insertion efficiency. The extension of the dimension of the hole as a function of the internal energy is discussed later on.

TABLE II. Degree of insertion and average energies transferred, in eV, as a function of internal energy for 10 000 trajectories. $T_{rot}=1200$ K; $E_{trans}=10$ eV.

E_{vib}, eV	N_{in}[a]	N_e[b]	$\langle\Delta E\rangle_{all}$	$\langle\Delta E\rangle_d$	$\langle\Delta E\rangle_{up}$
3.1	13	-	3.64	−0.01	3.88
5	11	1	3.63	−0.01	3.92
15	11	-	3.60	−0.03	3.94
20	11	-	3.58	−0.04	3.94
26	16	-	3.71	−0.05	4.14
35	9	-	3.55	−0.07	3.96

[a]Number of insertions including the number of escapes from the cage.
[b]Number of ions escaping the cage after insertion.

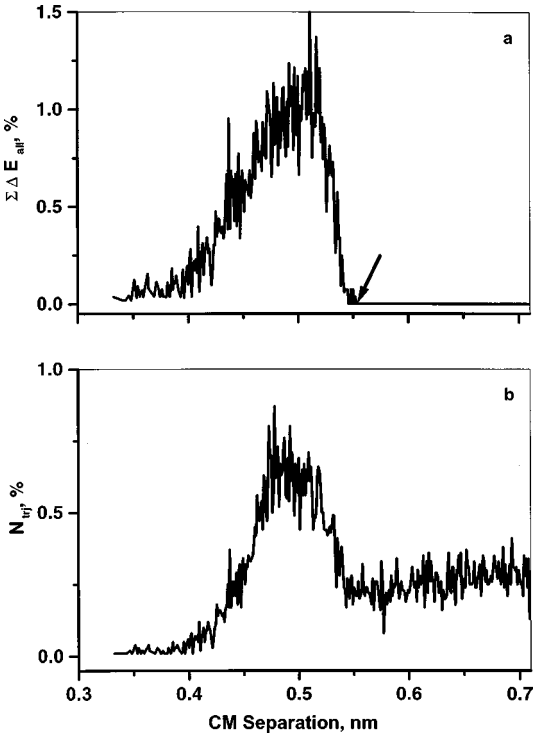

FIG. 3. (a) The percent energy transferred vs the distance of closest approach in a collision in center-of-mass coordinate system. (b) Percent trajectories vs the least center-of-mass distance. The total number of trajectories was 10 000 and the temperature was 613 K. The arrow indicates the cut-off point.

Collisional energy transfer probability density function, $P(E',E)$

Obtaining important dynamical information requires knowledge of $P(E',E)$. A new method of obtaining $P(E',E)$ was discussed recently by us[8f] and outlined in the theory section. The ability to obtain a reliable energy transfer probability density function depends very much on the ability to distinguish between effective and ineffective trajectories and thus obtain a reliable N_{eff}. To do so, ΔE is plotted versus both the least minimal distance and the least center of mass distance, LCM. For the sake of brevity, we report only on the LCM results. The first step in constructing $P(E',E)$ is to find a value of LCM above which no energy transfer takes place; Fig. 3(a). This cutoff value is then used to sort the trajectories and to determine the value of N_{eff}. The cutoff can be seen in Fig. 3(b) where all the trajectories below r_c belong to N_{eff}. For the case of 3.1 eV internal energy and 20 eV translational energy, as in the experiments of Anderson *et al.*,[2] N_{eff} is 29 600 out of a total of 50 000 trajectories. N_{eff} is then used in Eq. (3) to give the desired $P(E',E)$. The method leads to a $P(E',E)$ function which is normalized and detailed balanced. Figure 4 shows a sample $P(E',E)$ for the above experimental conditions. The $P(E',E)$ function is up-collision biased since the internal energy per mode is negligible compared with the translational energy and up-collision prevail. The shape of $P(E',E)$ is very unusual (Fig. 4) and was never found in previous trajectory calculations where a double exponential fit was sufficient and gave excellent results. There is the expected peak at low values of ΔE, but at higher values the tail of the up-collision side is practically

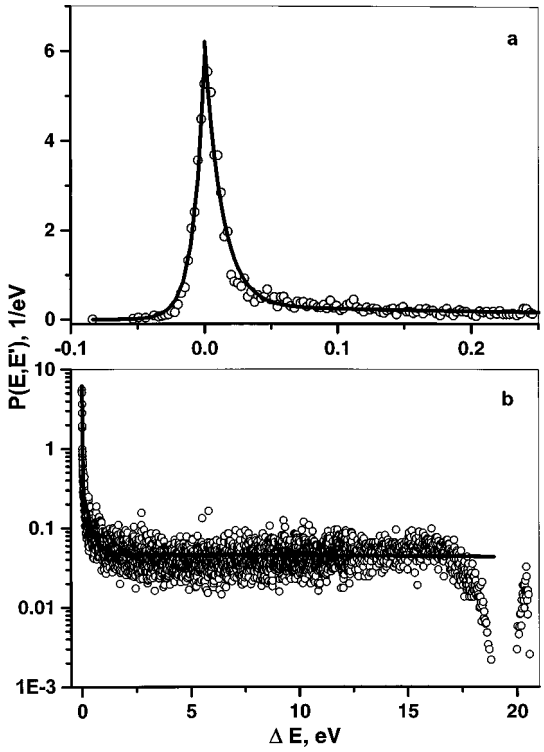

FIG. 4. Energy transfer probability density as a function of the amount of energy transferred in a collision. 50 000 trajectories were used. The temperature was 613 K, the translational energy was 20 eV and the number of effective trajectories was 29 600. (a) The high-energy peak. (b) The whole function on a logarithmic scale. The solid lines are best fit to the data.

flat with a slight upward slope. At very high ΔE there is a decrease in the function and then a rise that is due to endohedral events. The endohedral part occurs above the maximum kinetic energy of 20 eV. This is so because the energy of the system includes the intermolecular potential energy that is around 1 eV. Best fit to the data is obtained by using a double exponential function for the low-energy up and down parts and a linear fit to the long up-collision high-energy tail. The endohedral events were excluded from the function since only collisional events not leading to insertion are considered. The probability density function is give by:

$$P(E',E)=a\cdot\exp(-(\Delta E)/c)+b\cdot\exp(-(\Delta E)/d)+f\cdot(\Delta E)+g, \quad (4)$$

where $\Delta E=E'-E$. The values of the parameters are given in Table III.

Figure 4 agrees qualitatively with the $P(E',E)$ curve suggested by Anderson *et al.*[2c] to explain their experimental results for rare gas ions/C_{60} collisions. Their probability curve has an initial peak, a flat, long tail and a final endohedral peak. Our probability curve has the same gross features. Even though the details of M^+ and Rg^+ collisions with C_{60} are different, the main features should be the same and this is the root of the similarity between our M^+ results and Anderson's Rg^+ results. The 50 000 trajectories used in our calculations are a large enough sample and that ensures that the results are reliable and that the major features of this unusual shape of $P(E',E)$ are real.

Average energy transferred per collision, $\langle\Delta E\rangle$

The average energy transferred in up, down and all collisions is found by the two expressions given below:

$$\langle\Delta E_j\rangle=\sum_{i=1}^{N_{\mathrm{eff},j}}\Delta E_{ij}/N_{\mathrm{eff},j}, \quad (5)$$

where $N_{\mathrm{eff},j}$ is the number of up, or down, or all effective trajectories. The various $\langle\Delta E\rangle$'s quantities are also calculated by using the fitted energy transfer probability density function[8d]

$$\langle\Delta E\rangle_j=\int\Delta E_j P(E',E)d\Delta E\Big/\int P(E',E)d\Delta E, \quad (6)$$

where j indicates up, down, or all. For down collisions the integration limits are 0 and the initial energy E, for up collisions they are E and infinity and for all collisions the limits are 0 and infinity. Agreement of the results from the two expressions to within few percent is required. In the present case the value of $\langle\Delta E\rangle_{\mathrm{all}}$ from trajectories is 7.42 eV and from Eq. (6) it is 8.03 eV. The 8% agreement is as good as can be expected considering the scatter of the data.

The dependence of $\langle\Delta E\rangle_j$ on the relative translational energy is given in Fig. 5 and in Table I. As can be seen, the down transition are constant independent of E_{tr}. The up transitions, on the other hand, are large and are E_{tr} dependent. This is to be expected since E_{tr} is high and the internal energy per mode is low so up-collisions must prevail. For example, at the conditions of the experiments of Anderson *et al.* the total internal energy is 3.1 eV and the energy per mode is 0.05 eV or less. Therefore, $\langle\Delta E\rangle_{\mathrm{all}}$ is positive and increases with E_{tr}. The correlation between $\langle\Delta E\rangle_j$ and the translational energy is given, in eV, by the expressions

$$\langle\Delta E\rangle_{\mathrm{all}}=0.323\pm0.080+(0.295\pm0.009)E_{\mathrm{tr}}+(2.86\pm0.167)10^{-3}E_{\mathrm{tr}}^2$$

TABLE III. Fitting parameters for $P(E',E)$, Eq. (4). The internal energy is 3.1 eV and the translational energy is 20 eV. The total number of trajectories is 50 000.

Collisions	a, $(\mathrm{cm}^{-1})^{-1}$	b, $(\mathrm{cm}^{-1})^{-1}$	c, cm^{-1}	d, cm^{-1}	f, $(\mathrm{cm}^{-1})^{-2}$	g, $(\mathrm{cm}^{-1})^{-1}$
up	7.3×10^{-4}	3×10^{-5}	1.05×10^{2}	2.36×10^{3}	-2.6×10^{-12}	5.83×10^{-6}
	$\pm3.6\times10^{-6}$	$\pm1.3\times10^{-6}$	±0.95	1.32×10^{2}	$\pm2.6\times10^{-12}$	$\pm2.0\times10^{-7}$
down	7.3×10^{-4}	4×10^{-5}	1.04×10^{2}	2.34×10^{3}	0	0
	$\pm2.0\times10^{-5}$	$\pm1\times10^{-5}$	±5.4	$\pm1.27\times10^{3}$		

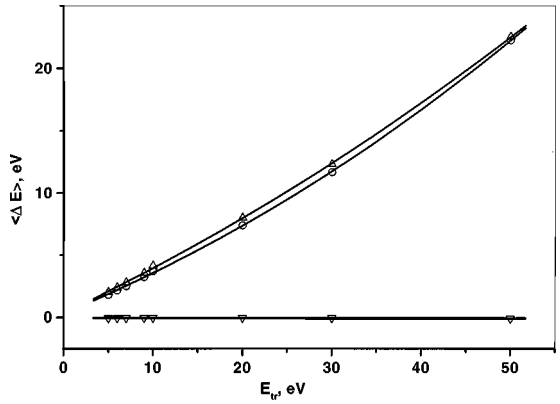

FIG. 5. The average energy transferred in up, down, and all collisions vs the translational energy. The lines are best fit to the data. 10 000 trajectories were used and the internal energy is 26 eV. Up (△), down (▽), all (○).

$$\langle \Delta E \rangle_u = 0.328 \pm 0.100 + (0.341 \pm 0.011) E_{\mathrm{tr}} + (2.00 \pm 0.206) 10^{-3} E_{\mathrm{tr}}^2. \quad (7)$$

The energy transfer process is practically independent of the rotational energy as can be seen by comparing Tables I and II. This is reasonable since rotations are very slow compared with the impact velocity obtained at the high translational energies used in the experiments and in our calculations.

The rate of dissociation of the collisionally excited C_{60}

The up-transitions are the vehicle by which C_{60} molecules are excited prior to decomposition. The rate coefficient for decomposition of a molecule with internal energy E which collides with an ion with relative translational energy E_{tr} and ends up with internal energy E' is

$$k = \int_{E0}^{\infty} k(E',J) P(E',E) dE', \quad (8)$$

where $k(E',J)$ is the rotational/vibrational energy dependent RRKM theory rate coefficient

$$k(E',J) = W(E^{\sharp},J)/\rho(E',J)/h, \quad (9)$$

where $W(E^{\sharp},J)$ is the number of states of the molecule in the transition state, $\rho(E',J)$ is the density of states of the excited molecule and h is Planck's constant. In the present case, the effect of rotations on the RRKM theory rate coefficient is small and therefore J will be omitted in future expressions (as will be low lying electronic states which may exist). k represents the rate coefficient for dissociation of all molecules excited by collisions with monoenergetic ions. It cannot, of course, be compared with thermal system.

The fraction, F, which remains after time t is given by

$$F = \exp(-kt), \quad (10)$$

where k is given by Eq. (8).

The density and number of states in Eq. (9) were calculated using experimental frequencies reported by Dresselhaus *et al.*[9a] and also by using frequencies calculated by us and by Stanton and Newton[9b] (after multiplying by 0.89). There was no substantial difference between the values of $k(E)$ calculated by using the different sets of frequencies. In practice, the experimental frequencies were used throughout this work. The reaction coordinate was chosen as the C–C stretching mode at 621 cm^{-1} and a C═C frequency was changed from 1426 in C_{60} to 1600 as in isolated propylene. These frequencies gave an Arrhenius factor of 4.36×10^{14} s^{-1}. Kolodney *et al.*[9c] treated the C_{60} molecule as its own heat bath and used a microcanonical system to obtain an experimental ''thermal'' rate coefficient with a frequency factor of 2.5×10^{13} s^{-1}.

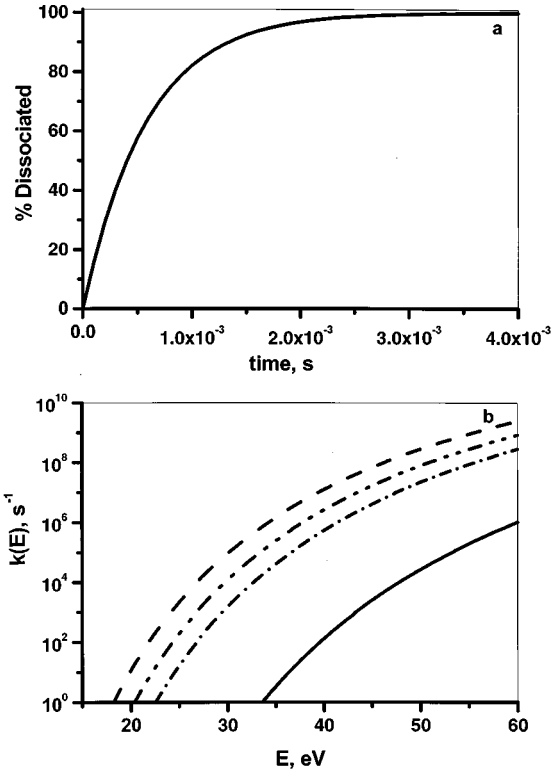

FIG. 6. (a) The percent dissociation of C_{60} excited by collisions with Li^+ as a function of time. $E_0 = 5.6$ eV, $E_{\mathrm{tr}} = 40$ eV, $k = 1.7 \times 10^3$, $t_{1/2} = 4.1 \times 10^{-4}$ s. (b) $k(E)$ vs internal energy. $E_0 = 4.8$ eV (---), $E_0 = 5.2$ eV (-·-·-), $E_0 = 5.6$ eV (-··-), $E_0 = 7.6$ eV (—).

The dependence of $k(E)$ on the energy in the range of 0–60 eV is shown in Fig. 6(b). $k(E)$ was calculated for four values of the threshold energy for dissociation E_0. The values of 4.8 eV[9h] and 7.6 eV[9f] are those reported for C_{60} dissociation and the values 5.2 eV[9d] and 5.6 eV[9e] were adopted from the values reported for C_{60}^+ ion dissociation. As can be seen there are orders of magnitude differences between the various values of the rate coefficient. The effects of the variations in the values of $k(E)$ on the rate coefficient for dissociation, k, [Eq. (8)] of an excited C_{60}^*

$$C_{60}^* \rightarrow C_{58} + C_2$$

are given in Table IV. As can be seen, the half-life of C_{60} varies greatly with the activation energy and with the translational energy. [The translational energy affects the $P(E',E)$ and provides a cutoff for the internal energy that the C_{60} can obtain via a collision with Li^+.] At translational energy of 20 eV the internal energies acquired by the molecule are too low for molecules to substantially dissociate on

TABLE IV. The overall rate coefficients and half-lives for the dissociation of C_{60} at two translational energies.

	$E_{tr}=20$ eV		$E_{tr}=40$ eV	
E_0, eV	k, s^{-1}	$t_{1/2}$, s	k, s^{-1}	$t_{1/2}$, s
4.8	4.3×10^{-1}	1.6	7.0×10^{4}	9.9×10^{-6}
5.2	2.06×10^{-2}	33.6	1.1×10^{4}	6.3×10^{-5}
5.6	9.38×10^{-4}	739.0	1.7×10^{3}	4.1×10^{-4}
7.6	6.17×10^{-11}	1.1×10^{10}	9.5×10^{-2}	7.3

a time scale of a mass spectrometric experiment. Even at the lowest activation energy it will take longer than 47 ms for 2% of the molecules[2e] to dissociate. A sample dissociation curve is provided in Fig. 6(a). At 40 eV translational energy, dissociation is fast at the lower activation energy but for $E_0=7.6$ eV it is still slow on mass spectrometric time scales. In a scattering experiment by Anderson and co-workers[2e] Li^+ is scattered off C_{60} gas. Our calculations show that in these experiments, some of the C_{60} molecules acquire enough energy to dissociate. In addition, since the C_{60} molecule has a low ionization potential of 7.6 eV, some excited molecules can ionize to give C_{60}^+. This is probably delayed ionization which emanates from statistically equilibrated molecules since direct charge transfer occurs with very low cross section[2c] because the ionization potential of Li is lower than that of the C_{60}. The two competing channels, dissociation and ionization, can affect the experimental results. The neutral, highly excited, C_{58} produced by the dissociation of C_{60} can further ionize by thermionic emission. In parallel, the hot C_{60}^+ ion can further dissociate to C_{58}^+ and C_2.

It is possible to apply the procedure given here for the dissociation of neutrals and for the dissociation of excited ions. $P(E',E)$ coupled with a (statistical) ionization model such as thermal emission model can give quantitative results for C_{60} ionization which can be compared with the appropriate experiment. It is clear that with the help of the scattering calculations reported here, it is possible to have an independent estimate of the amount of internal energy which C_{60} molecules acquire in collisions with charged ions.

The dynamics of intramolecular energy transfer

When an inelastic collision occurs, the sudden internal excitation of the C_{60} sets in motion an intramolecular dynamics that ends up in the molecule being ergodic. The nonmode-specific excitation of a moiety in the molecule by a collision involves a number of internal modes that in turn are coupled to additional modes. It is of great interest to determine the rate of intramolecular energy redistribution, IVR, for such a collisional event. We have monitored specific collisional events where the Li^+ hits the molecule at prespecified locations: a five-member ring, a double bond, a single bond, and a carbon atom. The criteria used to follow the temporal evolution of the excitation in the molecule are bond lengthening and energy contents in the stretchings and bendings at various geographic locations of the molecule. For example, the IVR dynamics of a five-member ring excitation was followed by observing the average lengths of the five

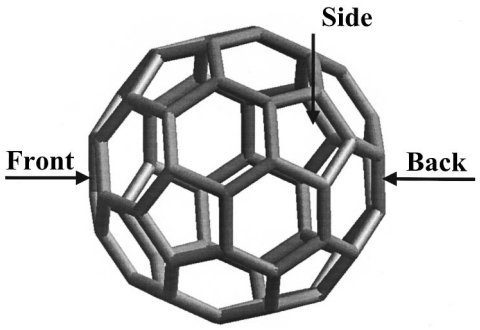

FIG. 7. A schematic drawing of a C_{60} molecule used in conjunction with studies of IVR. Front indicates the location of the impact of the Li^+ ion. Back indicates the opposite ring to the location of the front ring. Side indicates the side ring depicted in the drawing.

bonds in the ring being impacted (front), of the five bonds in the ring directly opposite to the front ring at the back of the molecule (back), and of the five bonds in the side rings (side) as a function of time (Fig. 7). In addition, the average energies in the five bonds of the rings were determined as a function of time. Figure 8 shows what happen when a collision with Li^+ with relative translational energy of 15 eV deposits 13.7 eV in a five-member ring of a C_{60} at 613 K. The initial spike [Fig. 8(a)] indicates the excitation of the stretches of the C–C bonds in the ring. This manifests itself in the lengthening of these bonds [Fig. 8(c)]. Excitation of

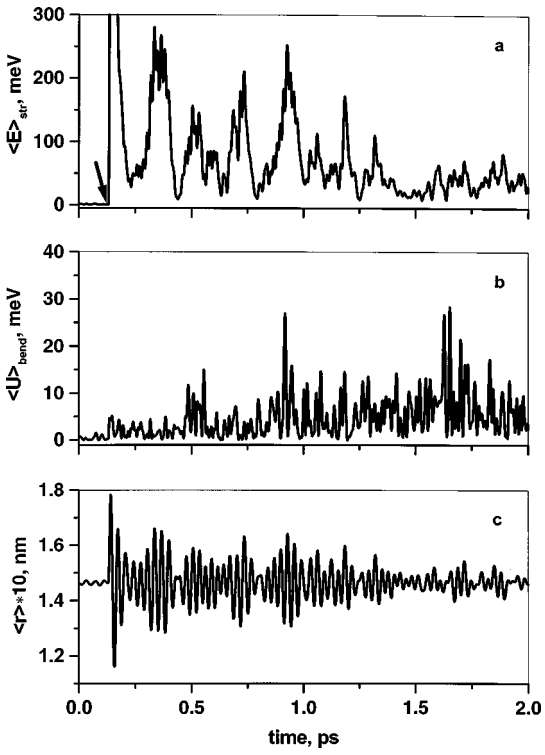

FIG. 8. (a) The average total energy in the stretches of the five-member ring whose center is hit by a Li^+ as a function of time. The truncated initial peak height is 800 meV and it indicates the beginning of the collision as does the arrow. (b) The average potential energy in the bends of the five-member ring as a function of time. (c) The average C–C bond length in the five-member ring as a function of time. The temperature is 300 K. The translational energy is 15 eV and the ΔE transferred is 13.7 eV. The total initial internal energy is 0.94 eV.

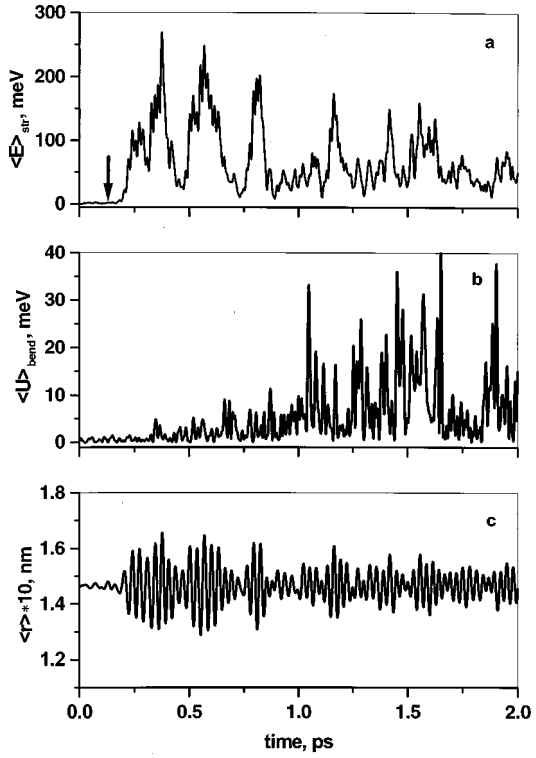

FIG. 9. (a) The average total energy in the stretches of the five-member ring opposite the ring whose center is hit by a Li^+ as a function of time. The arrow indicates the beginning of the collision. (b) The average potential energy in the bends of the five-member ring as a function of time. (c) The average C–C bond length in the five-member ring as a function of time. The temperature is 300 K. The translational energy is 15 eV and the ΔE transferred is 13.7 eV. The total initial internal energy is 0.94 eV.

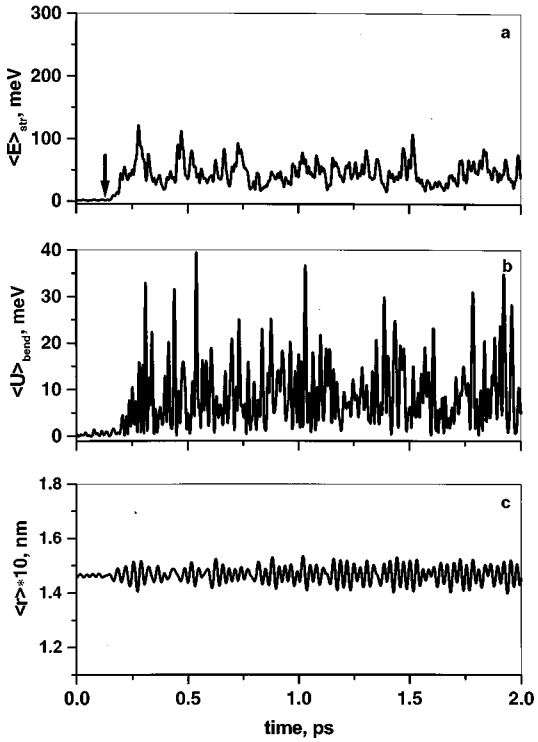

FIG. 10. (a) The average total energy in the stretches of the five-member ring on the far side of the ring whose center is hit by a Li^+ as a function of time. The arrow indicates the beginning of the collision. (b) The average potential energy in the bends of the five-member ring as a function of time. (c) The average C–C bond length in the five-member ring as a function of time. The temperature is 300 K. The translational energy is 15 eV and the ΔE transferred is 13.7 eV. The total initial internal energy is 0.94 eV.

the bends takes place much slower [Fig. 8(b)] and it develops over a fairly long period of time, 600 fs. The local excitation decays in ~1.5 ps.

Figure 9 shows what happens in the back ring. There is a ~67 fs time delay until the energy arrives in the local stretches which are then excited [Fig. 9(a) and 9(c)]. The bends follow with a longer time delay [Fig. 9(b)]. There is ''beating,'' excitation exchange, between back and front that slowly decays to a steady state. While the back and front rings are ''communicating'' with each other, the stretches in the side rings are hardly affected by the excitation (Fig. 10). There is excitation of course [Fig. 10(a) and 10(c)] but it is modest with little fluctuations and beatings. The bendings, on the other hand, are excited early, only 70 fs, after the stretches in the ring are first excited. This is in contrast to the situation in the front and back rings where the bends are relatively passive in the initial stage of the energy exchange.

The initial rate of IVR is extremely fast. Sixty-seven fs after the initial excitation of the front ring, energy appears in the back ring. This does not mean, of course, that the molecule is ergodic after this time, but it indicates that local clustering of energy in a molecule for an extended period of time is impossible. The beating between the front and back rings means that immediately after the impact an enlargement of the holes of the rings occurs on a periodic basis. This can facilitate insertion by consecutive collisions under conditions of high temperatures and pressures as is the case in the formation of inert-gas endohedral complexes in thermal systems.[1]

The rate of IVR is not a function of the relative translational energy or a function of the energy deposited in the molecule, ΔE, however, the details of the dynamics are. The beating between the two rings was much less pronounced when $\Delta E = 8.4$ eV was deposited than for the case when ΔE was 13.7 eV.

CONCLUSIONS

The present work gives an integrated picture of various processes that take place during a collision between a Li^+ ion and a C_{60} molecule. Using an intramolecular potential based on a sum of valence terms and nonbonded interactions which yields reliable force constants and a pairwise ion-molecule potential, the equations of motion were solved for a variety of initial conditions. The results of the trajectory calculations yield the following facts and observations:

(a) An average, global potential based on tens of thousands of trajectories is reported and a comparison is made between the fitting parameters derived for it and the parameters of the pairwise potential used in the calculations. It is shown that the two potentials are not interchangeable and the parameters of one cannot be used for the other.

(b) The number of endohedral complexes formed and the number of ions that escape the cage after entering it are reported as a function of the translational energy. The thresh-

old energy for the formation of $Li@C_{60}^{*}$ is 6 eV, in excellent agreement with experimental results. It is shown that the internal energy does not affect the insertion process that is dependent on the relative translational energy.

(c) Intermolecular energy transfer probability density function, $P(E',E)$ is calculated for 20 eV and 40 eV translational energies. The results of 50 000 trajectories are fitted to a continuous functions and the parameters are given. The shape of $P(E',E)$ is unusual. It has a long tail extending over all the energy range. It shows that, as expected, up-collisions prevail and that very large ΔE transfer are possible which can lead to dissociation of the C_{60} molecule.

(d) The dependence of the average energy transferred per collision $\langle \Delta E \rangle$ on the translational energy is linear up to 50 eV.

(e) Convoluting $P(E',E)$ with $k(E)$, the RRKM theory rate coefficient, the degree of dissociation of the molecule following collisional excitation was calculated.

(f) Following a collision impact in which energy is transferred to the molecule, redistribution of the internal energy occurs. We report on the dynamics of energy redistribution following an impact in which a pentagonal ring is excited. It is found that initially only subsets of mode are coupled to each other and that, initially, energy travels from one side of the molecule to another in ~67 fs. The energy content of the excited moiety decays in ~1.5 ps.

In summary, various outcomes of energetic collisions between a Li^{+} ion and a C_{60} molecule are reported. Insertion, endohedral formation and escape from the cage, energy transfer which causes internal excitation followed by dissociation, and intramolecular dynamics following an energy transferring collision are discussed. Where possible, comparisons with experiments are made.

ACKNOWLEDGMENTS

I.O. thanks Professor E. Kolodney for interesting discussions. This work is supported by the Fund for the Promotion of Research at the Technion to I.O. and by the Ministry of Science and the Arts.

[1] (a) M. Saunders, H. A. Jimenez-Vasques, R. J. Cross, and R. J. Poreda, Science **259**, 1428 (1993); (b) M. Saunders, H. A. Jimenez-Vasques, R. J. Cross, S. Mroczkowski, M. Cross, D. E. Giblin, and R. J. Poreda, J. Am. Chem. Soc. **116**, 2193 (1994); (c) M. Saunders, R. J. Cross, H. A. Jimenez-Vasques, R. Shimshi, and A. Khong, Science **271**, 1693 (1996).

[2] (a) Z. Wan, J. F. Christian, and S. L. Anderson, J. Chem. Phys. **96**, 3344 (1992); (b) J. F. Christian, Z. Wan, and S. L. Anderson, *ibid.* **99**, 3468 (1993); (c) Y. Basir and S. L. Anderson, *ibid.* **107**, 8370 (1997); (d) Z. Wan, J. F. Christian, and S. L. Anderson, Phys. Rev. Lett. **69**, 1352 (1992); (e) Z. Wan, J. F. Christian, Y. Basir, and S. L. Anderson, J. Chem. Phys. **99**, 5858 (1993).

[3] (a) T. Weiske, D. K. Bohme, J. Hrusak, W. Kratschmer, and H. Schwarz, Angew. Chem. **103**, 989 (1991); (b) Angew. Chem. Int. Ed. Engl. **30**, 884 (1991); (c) M. M. Ross and J. H. Callahan, J. Phys. Chem. **95**, 5720 (1991); (d) T. Wong, J. K. Terlouw, T. Weiske, and H. Schwarz, J. Mass. Spectrom. Ion Proc. **113**, 23 (1992); (e) R. C. Mowrey, M. Ross, and J. H. Callahan, J. Phys. Chem. **96**, 4755 (1992).

[4] (a) R. Shimshi, R. J. Cross, and M. Saunders, J. Am. Chem. Soc. **119**, 1163 (1997); (b) R. Tellgmann, N. Krawez, S. H. Lin, I. V. Hertel, and E. E. B. Campbell, Nature (London) **382**, 407 (1996).

[5] (a) L. Pang and F. Brisse, J. Phys. Chem. **97**, 8562 (1993); (b) S. Patchkovskii, and W. Thiel, J. Chem. Phys. **106**, 1796 (1997); (c) R. B. Darzynkiewicz and G. E. Scuseria, J. Phys. Chem. A **101**, 7141 (1997).

[6] (a) D. W. Brenner, Phys. Rev. B **42**, 9458 (1990); (b) J. Breton, J. Gonzales-Platas, and C. Girardet, J. Chem. Phys. **99**, 4036 (1993); (c) P. Procacci, G. Cardini, P. Salvi, and V. Schettino, Chem. Phys. Lett. **195**, 347 (1992).

[7] (a) T. Kaplan, M. Rasolt, M. Karimi, and M. Mostoller, J. Phys. Chem. **97**, 6124 (1993).

[8] (a) V. Bernshtein, K. F. Lim, and I. Oref, J. Phys. Chem. **99**, 4531 (1995); (b) D. C. Clary, R. G. Gilbert, V. Bernshtein, and I. Oref, Faraday Discuss. **102**, 423 (1995); (c) Venus, Quantum Chemistry Program Exchange by W. L. Hase, R. J. Duchovic, X. Hu, K. F. Lim, D. H. Lu, G. Pesherbe, K. N. Swamy, S. R. Vande-Linde, and R. J. Rolf, Quantum Chemistry Program, Exchange Bull; (d) V. Bernshtein and I. Oref, J. Chem. Phys. **108**, 3543 (1997); (e) V. Bernshtein and I. Oref, *ibid.* **106**, 7080 (1996); (f) **108**, 3543 (1998).

[9] (a) M. S. Dresselhaus, G. Dresselhaus, and P. C. Eklund, *Science of Fullerenes and Carbon Nanotubes* (Academic, New York, 1996); (b) R. E. Stanton and M. D. Newton, J. Phys. Chem. **92**, 2141 (1988); (c) E. Kolodney, B. Tsipinyuk, and A. Budrevitch, J. Chem. Phys. **102**, 9263 (1995); (d) C. Lifshitz, I. Gotkis, P. Sandler, and J. Laskin, Chem. Phys. Lett. **200**, 406 (1992); (e) P. Wurz and K. R. Lykke, J. Phys. Chem. **96**, 10129 (1992); (f) M. Foltin, M. Lezius, P. Scheier, and T. D. Mark, J. Chem. Phys. **98**, 9624 (1993); (g) I. Oref and D. W. Tardy, Chem. Rev. **90**, 1407 (1990); (h) E. Kolodney, B. Tsipinyuk, and A. Budrevitch, J. Chem. Phys. **108**, 5165 (1998).